

# A Stable Tracking Control of Skid Steered Mobile Platform

Seungwoo Jeon<sup>1</sup>, Wootae Jeong<sup>2</sup> and Duckshin Park<sup>2</sup>

<sup>1</sup>Department of Virtual Engineering, Korea University of Science and Technology, Daejeon, Korea

<sup>2</sup>Eco-Transport Research Division, Korea Railroad Research Institute, Gyeonggi-do, Uiwang, Korea

**Keywords:** Mobile Platform, Skid Steering, Trajectory Tracking, Driving Control, Vehicle Control.

**Abstract:** The skid steering technique has been widely used in controlling mobile vehicles without steering wheels because of light-weight and relatively simple structural configuration for steering motion control. However, since the skid controlled mobile platform system is based on nonholonomic constraint, it is essential to linearizing the nonlinear dynamic model of the vehicle for improving the stability of traction control. Recently developed ventilation duct cleaning robot with moving brushing arm also utilizes the skid steering system for traction control. Since the moving brush arm may change the mass center of the platform and effect on dynamics consequently, a new control scheme is suggested and simulated to achieve the stable trajectory tracking and driving motion of the developed mobile platform.

## 1 INTRODUCTION

Wheeled mobile platform with skid steering system is widely used in various industrial applications (Kanayama, Samson, Sampei *et al*, 1991). Skid steering helps the mobile platform without steering wheels to change the direction by assigning velocity difference between two side wheels (Fukao *et al*, 2000). Therefore, the skid steered platform can reduce the overall weight of the platform by removing mechanical steering parts and reduce the radius of rotation as well. However, due to the nonholonomic constraints in system characteristics, the lateral velocity of the mobile platform could not be controlled directly by the actuator. Therefore, many studies have been focused on linearizing the nonlinear mobile platform model for effective direction control based on speed difference of each side of wheels and Instantaneous Center of Rotation (ICR), or using various nonlinear control algorithms. According to Shojaei *et al*, to remove uncertainty caused by nonholonomic constraint in trajectory tracking control for wheeled robot without measuring speed, the control algorithm is presented concerning about the actuator dynamics. Also, in case of controlling the plant uncertainty and unmodeled dynamics, the control law using dual adaptive neural network algorithm has been suggested to improve trajectory-tracking ability (Marvin *et al*, 2009). Various control algorithm in

estimating contact force between tracked wheel and the road has been studied by (Bekker, 1969) and (Wong, 2001), whereas having the possibility of generating error because of heavy calculation. In addition, combined solution between kinematics and dynamic characteristics was investigated for driving control of wheeled robot to follow the reference path (Caracciolo *et al*, 1999). In case of controlling mobile platform with moving brush arm, the external force model has been investigated at the contact plane between rolling brush and cleaning surface (Jeong *et al*, 2013). It was not been considered the additional force is exerted by the manipulator when the platform is controlled to follow a designated path. In this paper, the control method is suggested to stable trajectory tracking when external force is exerted and dynamic model is investigated with the ventilation duct cleaning robot, which has overloaded moving arm on the platform.

## 2 KINEMATIC AND DYNAMIC MODELING

Figure 1 shows the free body diagram of the mobile platform. In the modelling, side effects by suspensions The mobile platform has a plane motion (moving on X-Y coordinate).

- The point contact occurs between wheels and the ground.

- Longitudinal wheel slip is neglected.
- Lateral force at the tire is generated by its vertical load and lateral friction coefficient.
- The speed of two wheels at each side are the same.

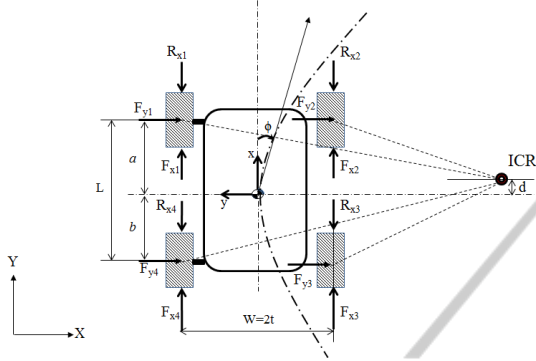


Figure 1: A schematic model of the mobile platform on a horizontal plane.

## 2.1 Dynamic Modelling of the Mobile Platform

Based on the schematic model of the mobile platform illustrated in Figure 1, the equation of motion of the platform can be given by

$$\begin{aligned} ma_x &= F_{x1} + F_{x2} + F_{x3} + F_{x4} - R_{x1} - R_{x2} - R_{x3} - R_{x4}, \\ ma_y &= -(F_{y1} + F_{y2} + F_{y3} + F_{y4}), \\ I\ddot{\phi} &= 2t(F_{x1} - F_{x2}) - M_r, \end{aligned} \quad (1)$$

where  $F_{xi}$  is the tractive force at the contact patch of the wheel,  $R_{xi}$  is the longitudinal resistive force of the wheel,  $F_{yi}$  is the lateral force at the contact patch of the wheel (Caracciolo *et al*, 1999). The resistive force, lateral force, and resistive moment at the Center of the Mass (CM) is calculated using friction coefficient ( $\mu_x, \mu_y$ ) by

$$R_x = \sum_{i=1}^4 R_{xi} = \mu_x \frac{mg}{4} (\text{sgn}(\dot{x}_1) + \text{sgn}(\dot{x}_2) + \text{sgn}(\dot{x}_3) + \text{sgn}(\dot{x}_4)), \quad (2)$$

$$F_y = \sum_{i=1}^4 F_{yi} = \mu_y \frac{mg}{a+b} (\text{sgn}(\dot{y}_1) + \text{sgn}(\dot{y}_3)), \quad (3)$$

$$M_r = a(F_{y1} + F_{y2}) - b(F_{y3} + F_{y4}) + \frac{w}{2} [(R_{x2} + R_{x3}) - (R_{x1} + R_{x4})]. \quad (4)$$

The dynamic model of the platform can be expressed with generalized coordinates,  $q = (X, Y, \phi)$ , and matrix form as follows

$$\begin{aligned} M &= \begin{bmatrix} m & 0 & 0 \\ 0 & m & 0 \\ 0 & 0 & I \end{bmatrix}, \quad c(q, \dot{q}) = \begin{bmatrix} R_x \cos\theta - F_y \sin\theta \\ R_x \sin\theta + F_y \cos\theta \\ M_r \end{bmatrix} \\ E(q) &= \begin{bmatrix} \cos\theta & \cos\theta \\ r & r \\ \sin\theta & \sin\theta \\ r & r \\ t & t \\ r & -r \end{bmatrix}, \quad \tau = 2rF_{xi} (i = 1, 2) \\ M\ddot{q} + c(q, \dot{q}) &= E(q)\tau, \end{aligned} \quad (5)$$

where  $r$  is the wheel radius,  $\tau_i$  are the torques at left and right side of motors to drive wheels, respectively.

To enable the skid steering and control of the platform, the longitudinal distance,  $d$ , between CM and the Instantaneous Center of Rotation (ICR) must be less than the distance,  $a$ , between the CM and front axle of wheels (see Figure 1, Caracciolo *et al*, 1999). Thus, constraint can be applied as

$$\dot{y} + d\dot{\phi} = 0, \quad 0 < d < a,$$

or, described with generalized coordinate as

$$[-\sin\phi \quad \cos\phi \quad d] \begin{bmatrix} \dot{X} \\ \dot{Y} \\ \dot{\phi} \end{bmatrix} = A(q)\dot{q} = 0. \quad (8)$$

Consequently, the platform motion dynamics becomes

$$M\ddot{q} + c(q, \dot{q}) = E(q)\tau + A^T(q)\lambda, \quad (9)$$

$$\dot{q} = V(q)p, \quad p \in R^2, \quad (10)$$

$$V(q) = \begin{bmatrix} \sin\phi & -\cos\phi \\ \sin\phi & \cos\phi \\ 0 & -\frac{1}{d} \end{bmatrix}, \quad (11)$$

where  $\lambda$  is the Lagrange multipliers,  $p$  is a pseudo-velocity and  $V(q)$  is  $3 \times 2$  matrix for coordinate transformation. By differentiating Equation (10) and eliminating  $\lambda$  from Equation (9), the dynamic model can be reduced as following

$$\dot{q} = Vp,$$

$$\dot{p} = (V^T M V)^{-1} V^T (E\tau - M\dot{V}p - c) \quad (12)$$

Based on the Equation (9), the state feedback control law is given by

$$\tau = (V^T E)^{-1} (V^T M V u + V^T M \dot{V} p + V^T c), \quad (13)$$

where  $u = (u_1, u_2)$  is the vector of control variable and the system will be a second-order kinematic model.

The output position of the robotic platform is represented as

$$z(t) = \begin{bmatrix} X + d\cos\phi \\ Y + d\sin\phi \end{bmatrix} \quad (14)$$

Also, to apply dynamic state feedback to trajectory tracking control, an integrator on the input  $u_1$  is introduced as

$$\begin{aligned} u_1 &= \kappa, \\ \dot{\kappa} &= v_1, \\ u_2 &= v_2, \end{aligned} \quad (15)$$

where  $\kappa$  is the controller state and  $v_1, v_2$  are the control inputs.

By applying input-output decoupling algorithm (see [13]) and differentiating the Equation (14) until the control input  $v$  is appeared, the equation can be written as

$$\begin{aligned} \ddot{z} &= \begin{bmatrix} \cos\phi & \frac{p_1}{d}\sin\phi \\ \sin\phi & \frac{p_1}{d}\cos\phi \end{bmatrix} v + \begin{bmatrix} \frac{2\kappa p_2 \sin\phi}{d} - \frac{p_1 p_2^2 \cos\phi}{d^2} \\ -\frac{2\kappa p_2 \cos\phi}{d} - \frac{p_1 p_2^2 \sin\phi}{d^2} \end{bmatrix} \\ &= \alpha(q, p)v + \beta(q, p). \end{aligned} \quad (16)$$

To avoid singularity for the matrix  $\alpha$ , it is assumed that the longitudinal velocity of the platform  $p_1$  is not equal to zero. Thus, the control law is expressed as

$$v = \alpha^{-1}(q, p)[R - \beta(q, p)], \quad (17)$$

where  $R$  is the trajectory jerk reference, yielding

$$\ddot{z} = R. \quad (18)$$

The input  $R_i$  ( $i=1,2$ ) can be expressed as

$$R_i = \ddot{z}_{di} + k_{ai}(\ddot{z}_{di} - \ddot{z}_i) + k_{vi}(\dot{z}_{di} - \dot{z}_i) + k_{pi}(z_{di} - z_i), \quad (19)$$

where the gains are such that  $\lambda^3 + k_{ai}\lambda^2 + k_{vi}\lambda + k_{pi}$  ( $i = 1, 2$ ) Hurwitz polynomials,  $z_d$  is the desired reference trajectory and  $z, \dot{z}$  and  $\ddot{z}$  can be calculated in terms of  $q, p$ , and  $\kappa$  (De Luca, 1998).

## 2.2 Dynamic Modelling of the Rotating Brush Arm

As depicted in Figure 2, the rubbing motion of the rolling brush arm covers two side surfaces and upper surface of the ventilation duct. When the brush contacts with side surfaces (CASE I), the vertical forces and geometric relationship under surface friction are illustrated in Figure 2.

When the brush meets the surface of the duct, reaction force ( $F_s$ ) and friction force ( $T$ ) act as resistance forces in cleaning process. Also,  $F_s$  and  $T$  enforce additional forces to the wheels of the mobile

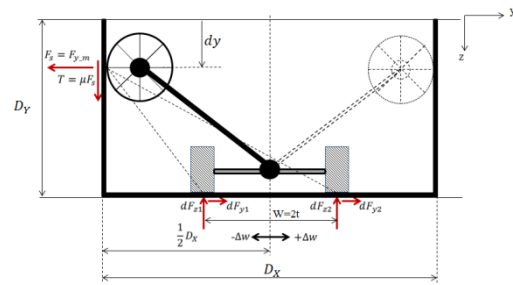


Figure 2: A schematic of forces exerted on target surfaces from brushing arm and mobile platform.

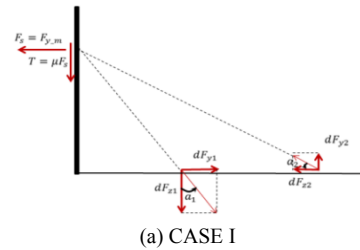
platform. The force equilibrium equation between wheels and surface is given by

$$\sum F_z = 0; T = \mu F_s = 2dF_{z1} + 2dF_{z2}, \quad (20)$$

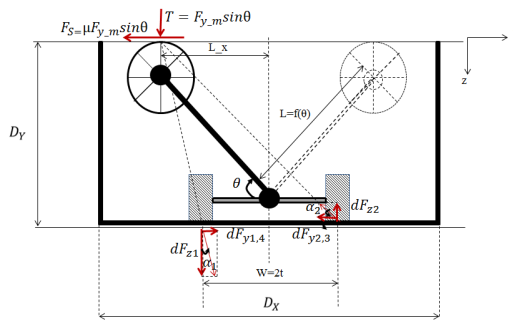
$$\sum F_y = 0; F_s = F_{y,m} = 2dF_{y1} + 2dF_{y2}, \quad (21)$$

$$\sum M_G = 0; 2dF_{z1} \left( \frac{D_x - W}{2} \right) + 2dF_{z2} \left( \frac{D_x + W}{2} \right) = 0 \quad (22)$$

In a case of upper surface cleaning motion, the interaction forces between the wheel and the rolling brush (CASE II) is illustrated in Figure 3. The difference between CASE I and CASE II is the direction of vertical forces on the cleaning surface and platform wheels. Since the direction of interacting forces in two cleaning positions of the brushed arm, control forces have to be calculated by considering different directions of each reacting forces from surfaces.



(a) CASE I



(b) CASE II

Figure 3: Free body diagram of interacting forces between the platform and target surfaces.

The vertical load and the lateral force divided by

wheels and the road interaction as shown in Figure 3 can be calculated as

$$\text{CASE I: } dF_{z1} = \frac{F_s(D_x+W)}{W}, dF_{z2} = -\frac{\mu F_s(D_x-W)}{W},$$

$$dF_y = \left[ \frac{dF_{z1}}{2\tan(\alpha_1)} \frac{dF_{z2}}{2\tan(\alpha_2)} \frac{dF_{z2}}{2\tan(\alpha_2)} \frac{dF_{z1}}{2\tan(\alpha_1)} \right]^T, \quad (23)$$

$$\text{CASE II: } dF_{z1} = \frac{\mu F_s(-D_y - L_x + W)}{\mu W},$$

$$dF_{z2} = \frac{\mu F_s(-D_y - L_x - W)}{\mu W}, \quad (24)$$

$$dF_y = \left[ \frac{dF_{z1}}{2\tan(\alpha_1')} \frac{dF_{z2}}{2\tan(\alpha_2')} \frac{dF_{z2}}{2\tan(\alpha_2')} \frac{dF_{z1}}{2\tan(\alpha_1')} \right]^T.$$

The angle  $\alpha_1$  and  $\alpha_2$  are given by

$$\alpha_1 = \tan^{-1} \left( \frac{D_y - dy}{\frac{D_x}{2} - t - \Delta w} \right), \alpha_2 = \tan^{-1} \left( \frac{D_y - dy}{\frac{D_x}{2} + t + \Delta w} \right), \quad (25)$$

$$\alpha_1' = \tan^{-1} \left( \frac{D_y - dy}{L_x - t - \Delta w} \right), \alpha_2' = \tan^{-1} \left( \frac{D_y - dy}{L_x + t + \Delta w} \right),$$

where  $\Delta w$  is the position change of the mobile platform,  $dy$  is the vertical change of the brush position, and  $D_x$ ,  $D_y$  is the dimension of the rectangular duct. The tangential force generated by pressurizing and scrubbing the duct surface influences traction forces of the both wheels. However, since responding force on each wheel is different, motor torques for controlling each wheel have to be calculated independently for increasing control stability of the mobile platform. According to the Equation (2), traction exerted to the wheel can be decided by the magnitude of the load.

In braking, it is required to consider direction of motor torque because there exist negative loads and traction forces for each wheel. To resolve this problem, it is also assumed that the lifting effect by negative force on the wheel is zero traction force.

Considering the forces acting on wheels overloaded by rolling brush during cleaning motion of the arm, the reaction forces of  $c(q, \dot{q})$  in Equation (5) can be rewritten as

$$c(q, \dot{q}) = \begin{bmatrix} (R_x + \bar{R}_x) \cos \phi - (F_y + \bar{F}_y) \sin \phi \\ (R_x + \bar{R}_x) \sin \phi + (F_y + \bar{F}_y) \cos \phi \\ M_r + \bar{M}_r \end{bmatrix}, \quad (26)$$

$$\bar{R}_x = \mu_x (dF_{z1} + dF_{z2}), \quad (27)$$

$$\bar{F}_y = \sum_{i=1}^4 dF_{yi}, \quad (28)$$

$$\bar{M}_r = a(dF_{y1} + dF_{y2}) - b(dF_{y3} + dF_{y4}) + \left( \frac{W}{2} + \Delta w \right) (dF_{z2}) - \left( \frac{W}{2} - \Delta w \right) (dF_{z1}), \quad (29)$$

where

$\bar{R}_x$  is the sum of extra longitudinal forces at wheels,  $\bar{F}_y$  is the sum of extra lateral forces at wheels,

$\bar{M}_r$  is the moment generated by additional forces.

## 2.3 Kinematic Analysis of the Rotating Brush Arm

With a simple five link-mechanism, workspace of the rolling brush can be analysed as shown in Figure 4. However, for the simplicity of mechanism and control, the linkage can be modelled with a prismatic link and a revolute joint as depicted in Figure 5.

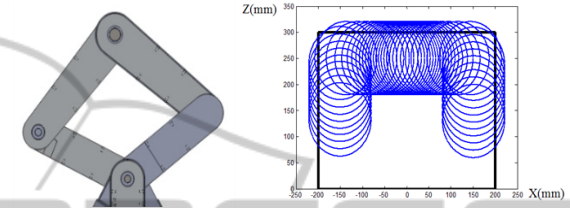


Figure 4: Workspace of the 5 link manipulator with rolling brush.

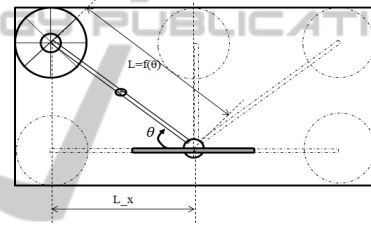


Figure 5: Simplified kinematic model of robotic arm.

As depicted in Figure 5, the length of the link becomes a function of the rotation angle ( $\theta$ ) whose workspace can be expressed by following function. The pushing force acting by the link can be modelled as illustrated in Figure 6.

$$L(\theta) = \begin{cases} \frac{\frac{1}{2}D_x}{\cos\theta} & : 0 \leq \theta \leq \tan^{-1} \left( \frac{D_y}{\frac{1}{2}D_x} \right) \\ \frac{D_y}{\sin\theta} & : \tan^{-1} \left( \frac{D_y}{\frac{1}{2}D_x} \right) \leq \theta \leq \pi - \tan^{-1} \left( \frac{D_y}{\frac{1}{2}D_x} \right) \end{cases}, \quad (30)$$

$$L_x = \begin{cases} \frac{1}{2}D_x & : 0 \leq \theta \leq \tan^{-1} \left( \frac{D_y}{\frac{1}{2}D_x} \right) \\ L \cos\theta & : \tan^{-1} \left( \frac{D_y}{\frac{1}{2}D_x} \right) \leq \theta \leq \pi - \tan^{-1} \left( \frac{D_y}{\frac{1}{2}D_x} \right) \end{cases}$$

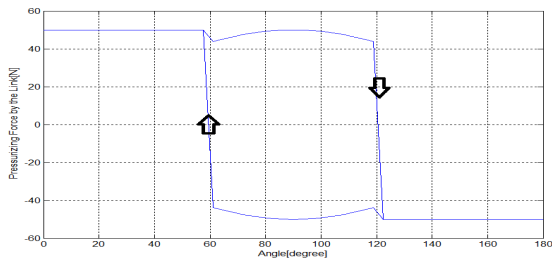


Figure 6: Duration of the load applied by using simplified model of variable length of the link with rolling brush.

### 3 SIMULATION AND RESULTS

The control algorithm for stable trajectory tracking presented in section 2 has been simulated with a MATLAB™ tool. Based on the prototype of duct cleaning robot as shown in Figure 7, mechanical parameters in simulation are selected and summarized in Table 1.

Table 1: Summary of the mobile platform model.

Length (L)	0.30 [m]
Distance from C.M to front axle(a)	0.15 [m]
Distance from C.M to rear axle (b)	0.15 [m]
Track Width (W)	0.23 [m]
Radius of wheel (r)	0.05 [m]
Overall mass of Duct cleaning robot	7.823[kg]
Inertia of the platform	0.19 [kgm <sup>2</sup> ]
Mass of the manipulator	1.777 [kg]



Figure 7: Prototype of the duct cleaning robot.

The desired trajectory is  $z_{d1} = 0.05t, z_{d2} = 0.05t$  as a straight line whose angle in the view of absolute coordinates is  $\theta = 45[\text{deg}]$  for  $t \in [0,60\text{sec}]$ . The speed of the mobile platform was set to 0.05m/s and the period of the cyclic motion traveling arms to clean both sides of the duct is 1 second. To prevent singularity of the equation of motions, the initial velocities and angular velocity of the platform should not be zero (Yang *et al*, 1999). The friction coefficients of duct surfaces are set to  $\mu_x = 0.895$  and  $\mu_y = \mu = 0.1$ , respectively. The initial velocity

of wheels is 0.01m/s and the initial angular velocity at CM is set to 0.02 rad/sec.

The load caused by the link with rolling brush is set to 50[N] with iterative calculation to keep stability of moving platform. The simple motor model has used whose torque saturation limit is set as 0.5 [Nm]. In order to track the reference path, the parameters of Equation (19) are chosen as  $k_a = 4, k_v = 28, k_p = 75$  to minimize tracking error (De Luca, 1998).

Simulation results for trajectory tracking of the mobile platform are shown in Figure 8. The position errors of longitudinal and lateral direction were controlled within 4mm shown in Figure 8(c) and (d). It is also considered that lateral forces were exerted at four wheels against the load by the link with rolling brush to surface planes. The mobile platform was controlled to sustain posture with two actuators under the changing lateral loads on wheels. Additional method in tracking against the lateral load is required to reduce the magnitude of the fluctuated error.

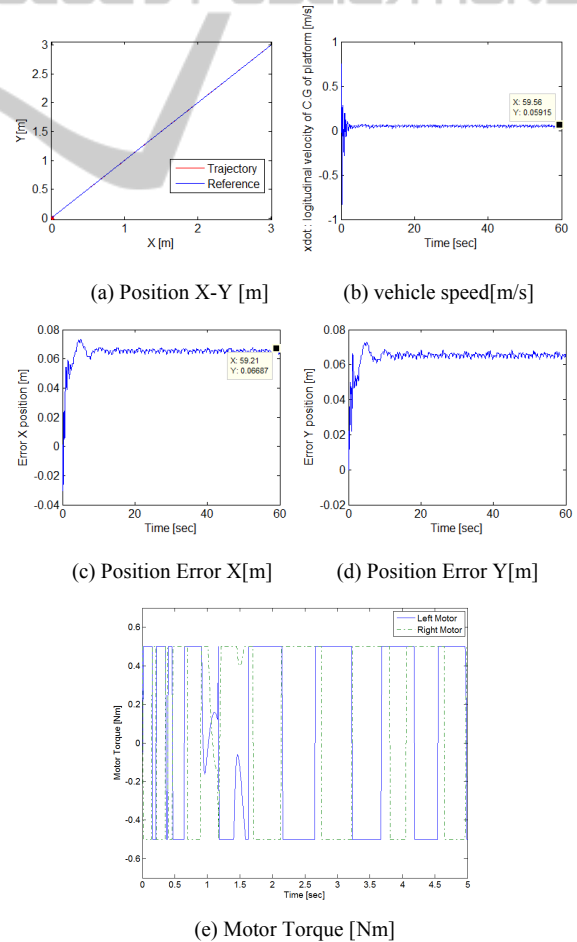


Figure 8: Simulation results for trajectory tracking.

## 4 CONCLUSIONS

A dynamic trajectory tracking controller in the application of moving arm with rolling brush has proposed for skid steered mobile platform. Considering nonholonomic constraint with skidding wheels, the controller consists of proportional terms with kinematic elements (e.g. position, velocity, acceleration) of the platform. A nonlinear characteristics concerning about tire deformation has been neglected by considering the lateral friction coefficient as a constant. Simulation results indicate that the mobile platform can be skid-controlled under external force. However, when the external force over 50N was enforced, the controller should be modified to minimize the position error of the platform.

## ACKNOWLEDGEMENTS

This research was carried out as a part of project (13RTRP-B069116-01) partially funded by the Ministry of Land, Infrastructure and Transport and Ministry of Science, ICT and Future Planning in Korea.

## REFERENCES

- Kanayama, Y., Kimura, Y., Miyazaki, F., Noguchi, T., 1991. A stable tracking control method for a nonholonomic mobile robot. *IEEE/RSJ Int. Workshop Intelligent Robots and Systems*, pp.1236-1241.
- Samson, C., Ait-Abderrahim, K., 1991. Feedback control of a nonholonomic wheeled cart in Cartesian space. *in Proc. IEEE Int. Conf. Robotics and Automation*, pp.1136-1141.
- Sampei, M., Tamura, T., Itoh, T., Nakamichi, M., 1991. Path tracking control of trailer-like mobile robot. *in Proc. IEEE/RSJ Int. Workshop Intelligent Robots and Systems*, pp. 193-198.
- Fukao, T., Nakagawa, H., Adachi, N., 2000. Adaptive Tracking Control of a Nonholonomic Mobile Robot. *IEEE Transactions on Robotics and Automation*, Vol. 16(5), pp.609-615.
- Shojaei, K., Shahri, A. M., 2012. Output feedback tracking control of uncertain non-holonomic wheeled mobile robots: a dynamic surface control approach, *IET Control Theory and Applications*, Vol6(2), pp. 216-228.
- Marvin, K. B., Simon G. F., Liberato, C., 2009. Dual Adaptive Dynamic Control of Mobile Robots Using Neural Networks, *IEEE Trans. on Systems, Man, and Cybernetics*, Vol.39(1), pp. 129-141.
- Bekker, M. G., 1969. *Introduction to Terrain-Vehicle Systems*, Ann Arbor, MI: University of Michigan Press.
- Wong, J. Y., 2001. *Theory of ground vehicles*, John Wiley and Son, 3<sup>rd</sup> edition.
- Caracciolo, L., 1999. Trajectory Tracking Control of a Four-Wheel Differentially Driven Mobile Robot, *IEEE International Conference on Robotics and Automation*, pp.2632-2638. IEEE.
- Yi, J., Song, D., Zhang, J., Goodwin, Z., 2007. Adaptive Trajectory Tracking Control of Skid-Steered Mobile Robots, *IEEE Conference on Robotics and Automations*, pp.2605-2610. IEEE.
- Anthony, M., Jorge, L. M., Jesus, M., Jose, L. B., 2007. experimental kinematics for wheeled skid-steer mobile robots, *Proc. IEEE/RSJ Int. Conference of Intelligent Robots System*, San Diego, pp.1222-1227.
- Jeong, W., Jeon, S., Park, D., Kwon, S., 2013. Surface Cleaning Force Control of Rotating Brushes For an Air Duct Cleaning Robot, *International Conference on Informatics in Control, Automation and Robotics (ICINCO)*, pp. 453-457. SCITEPRESS.
- De Luca, A., Oriolo, G., Samson, C., 1998, Feedback control of a nonholonomic car-like robot, *in J. P. Laumond (Ed.) Robot Motion Planning and Control, Lecture Notes in Control and Information Sciences*, Vol. 229, pp.171-253, Springer-Verlag, London.
- Will, A. B., Zak, S. H., 1997. Modeling and control of an automated vehicle, *Vehicle System Dynamics*, Vol. 27, pp.131-155. SWETS AND ZEITLINGER.
- Yang, J., Kim, J., 1999. Sliding Mode Control for Trajectory Tracking of Nonholonomic Wheeled Mobile Robots, *IEEE Transactions on Robotics and Automation*, Vol. 15, No. 3, pp.578-587.